

**How to Cite:**

Bidkar, J. S., Bidkar, S. J., Dama, G. Y., Rao, M. E. B., & Bhambar, K. V. (2022). Development and modification of the natural polymers by converting them into nanobiocomposite. *International Journal of Health Sciences*, 6(S3), 3497–3507. <https://doi.org/10.53730/ijhs.v6nS3.6517>

# Development and modification of the natural polymers by converting them into nanobiocomposite

**Dr. Jayant S. Bidkar**

Sharadchandra Pawar College of Pharmacy, Otur, Pune  
Corresponding author email: [jayantbidkar@gmail.com](mailto:jayantbidkar@gmail.com)

**Shital J. Bidkar**

Sharadchandra Pawar College of Pharmacy, Otur, Pune

**Dr. Ganesh Y. Dama**

Sharadchandra Pawar College of Pharmacy, Otur, Pune

**Dr. M. E. Bhanoji Rao**

Calcutta Institute of Pharmaceutical Technology & Allied Health Sciences,  
Banitabile, Uluberia, Howrah, West Bengal

**Kunal V. Bhambar**

Mgv's Pharmacy College Panchavati, Nashik

**Abstract**--The main target of this study is to develop an antibacterial chitosan nanocomposite fabric among in situ crated silver nanoparticles utilizing Vitex leaf extract, which is a medicinal herb. The CNCFs were evaluated using scanning electron microscopy (SEM), Fourier transform infrared (FT-IR) spectroscopy, X-ray diffraction (XRD), and antimicrobial testing. Additionally, these CNCFs have excellent antibacterial characteristics. These CNCFs could be used in medical applications like surgical aprons, wound cleansing, wound dressing, and hospital bed materials, as they were manufactured utilising a simple and environmentally acceptable approach.

**Keywords**--natural polymer, chitosan textile, silver nanoparticles, nanobiocomposite.

## Introduction

Nanobiocomposite (NBC) materials have evolved as an alternative to standard materials, among probable attribute and success during a several applications in a variety of industries (aeronautical, automotive, furniture, packaging, transportation, medical, and defense). Nanobiocomposite materials are made up of two, three or more components, one of which is in the form of matrix and the others in the form of particles or biofibres. When a load is applied to nanobiocomposite materials, it is distributed evenly throughout all parts. The most significant advantages of polymerbased nanobiocomposite materials are enhanced industrial productivity, ease of processing technology and lower manufacturing prices [1-3].

The development of an infiltration network enclosed by the matrix is the most crucial property in the formulation of nanocomposites utilizing several classes of nanoparticles like nano clays, carbon nanotubes, or cellulose nanocrystals, (CNCs) [4]. Numerous investigations on the creation of advanced organic/inorganic hybrid substances and nanocomposites have been conducted [5]. "Nanocomposite" is a term that is frequently used for nanofiller filled polymers with distributed nanofillers. Particle sizes lower than 100 nanometers on average [6]. Polymers are a type of material that is made up of metal [6to9] and semimetal as a good host material [10to14] conductor nanoparticles, at the same time, optical and electrical qualities are outstanding. A valiant effort polymericinorganic nanocomposites are a type of polymerinorganic nanocomposites that have a variety of properties. Electrical, optical, and magnetic qualities that are fascinating are steadily superior to the center polymer or inorganic family has been described in the literature [15-18].

Metallic nanoparticles polymer nanocomposites can be made by adding the metal precursor to a polymer solution and then reducing it with a reducing agent or by thermolysis, or by polymerizing a colloid of metallic nanoparticles in a monomer solution and then reducing it, or by polymerizing a colloid of metallic nanoparticles in a monomer solution and then reducing it. stabilizers are important in the creation of metal nanoparticles because they influence both the formation and dispersion stability of the particles [19-21].

Chitosan is a deacetylated polysaccharide derived from natural chitin, which is found in crustacean shells and many fungi's cell walls. Chitosan has recently sparked a lot of attention as a possible polysaccharide resource because of its beneficial capabilities, like studies on mix films including chitosan based upon its biocompatibility, biodegradability, nontoxicity and adsorption properties [22-25]. Metal nanoparticles can be made from metal salts in a variety of ways, including chemical and biological approaches [26]. Many leaf extracts are currently being used to convert metal salts into their respective nanoparticles. To make silver nanoparticles and copper nanoparticles, reducing agents such as tea leaf and coffee powder, plant tea, *Ocimum sanctum*, and *Gymnema sylvestre* were utilized.

Several researchers disseminated the produced metal nanoparticles in polymer matrices to create polymer nanocomposites. Although, nanoparticle dispersion in polymer matrices frequently results in agglomeration [27]. To solve this problem, several researchers used several leaf extracts as reductant to make silver nanoparticles and copper nanoparticles in chitosan matrix in situ. The scientists attempted to generate silver nanoparticles in situ in chitosan textiles utilizing Vitex leaf extract as a reducing agent in this investigation.

The chitosan nanocomposite fabrics were examined using Fourier transform infrared (FTIR) spectroscopy, scanning electron microscopy (SEM), X-ray diffraction (XRD), and antibacterial action testing. The main goal of this research was to develop antibacterial chitosan fabrics among in situ generated silver nanoparticles during medical applications like surgical aprons, wound healing and wound cleaning materials and hospital bed spreads utilizing an easy and low cost process that used medicinal leaf extract as a reductant.

### **Material and Methods Materials**

Silver nitrate was purchased as an offering sample from Loba Chem, Mumbai, India, and rinsed twice among double distilled water before air drying. Vitex leaves were sourced from the surrounding region.

### **Methods**

The Vitex leaves were cleaned and cut towards little pieces prior to being added to distilled water at 80°C for 20 minutes. The empty was segregated, filtered, and stored until the next time it was needed. To manufacture CNCFs containing in situ produced silver nanoparticles, aqueous AgNO<sub>3</sub> solutions with concentrations of 1, 2, 3, 4, and 5 mmol/L were first created independently. The Vitex leaf extract was soaked in the cleaned chitosan, allowing the leaf extract to diffuse into the textile fibres. The leaf extract infused textile fibres were then stored in various concentrations of aq. AgNO<sub>3</sub> solutions. When these fibres were immersed in yellow brown, their hues gradually shifted and intensified. Behind 24 hours the CNCFs were properly cleansed among distilled water.

### **Characterization**

The FTIR spectra of chitosan and CNCFs with in situ generated silver nanoparticles were recorded on a smart iTR ATR Nicolet using 10 FTIR spectrophotometers in the range of 4000 to 500 cm<sup>-1</sup> with 32 scans in each case at a resolution of 4 cm<sup>-1</sup>. To investigate the presence of silver nitrite and its particle size distribution in the CNCFs, SEM pictures were acquired with a Zeiss EVO 18 scanning electron microscope at a 10 kV accelerating voltage. The X-ray diffraction spectra of the samples were recorded using the same instrument. The samples were gold sputter coated before being photographed. The XRD of the matrix and CNCFs containing in situ generated silver nitrite was recorded using a Bruker Eco D8 XRD

diffractometer in the  $2\theta$  range of  $10^\circ$  to  $90^\circ$ , a voltage of 40 kV, and a current of 25 mA. The disc method was used to test the matrix's antibacterial activity, and CNCFs with in situ produced silver nitrite were found to be effective against two gramme negative (*Pseudomonas* and *E. coli*) and two gramme positive (*Bassilus subtilis* and *Staphylococcus aureus*) bacteria. The inhibitory zones that were seen were photographed, and the diameter of each zone was measured.

## Result and Discussion

Figure 1 shows digital images of the chitosan fabric, matrix, and CNCFs generated with 15 mmol/L aq. silver nitrite solutions. As illustrated in Fig. 1, the chitosan fabric was yellow, whereas the Vitex leaf extract saturate textile fabric (matrix) was light brown. Instead, when the concentration of the source solution grew, the CNCFs' color shifted from medium brown to dark brown. Preliminarily, the in situ initiation of the silver nanoparticles in the matrix can be seen as a colour shift. The CNCFs' SEM images were documented in order to visualize the silver nanoparticles that were created. Figure 2 displays SEM images of CNCFs using aq. silver nitrite solutions with concentrations of 1 mmol/L (minimum) and 5 mmol/L (highest). The same graphic also includes the EDX spectra that were described at the same time as the paralleling SEM images. Micrographs were used to examine the particle size distribution in both of these occurrences, and the results are shown in the same image. In the SEM images in Figs. 2a and 2b, the spherical shape of the generated silver nanoparticles is clearly visible. The EDX spectra in figures 2c and 2d verified the presence of silver particles. The intensity of the EDX apex paralleling the silver element was also found to be higher when CNCF was made with a 5 mmol/L origin solution than when CNCF was formed with a 1 mmol/L origin solution. When a more concentrated origin solution was used, it appeared that a large number of silver nanoparticles were produced. Figures 2e and 2f show the particle size distribution of CNCFs generated using 1 mmol/L and 5 mmol/L origin solutions, respectively. The largest amount of created silver nanoparticles was in the particle range of 94–100 nm in both occurrences, as shown by the distribution curves. Although, in the CNCFs generated with 1 mmol/L and 5 mmol/L origin solutions, the average size of the formed silver nanoparticles was 89 nm and 104 nm, respectively. This could be due to the agglomeration of a few nanoparticles that occurred when highly concentrated origin solutions were employed. The average particle size of CNCFs generated using extra concentrated origin solutions (2, 3 and 4 mmol/L) was considered to be in the middle of these two values.



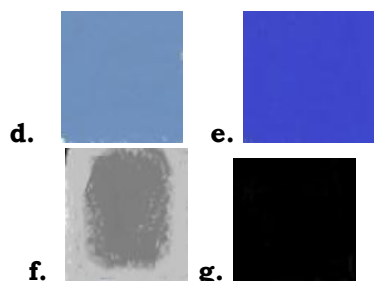


Fig. 1: CNCFs among in situ generated silver nanoparticles using 1 mmol/L (a); digital pictures of chitosan fabric (b); matrix (c) CNCFs among in situ generated silver nanoparticles using 1 mmol/L (c) (d) 2 mmol/L a concentration of 3 mmol/L (e) (f) 4 mmol/L and mmol/L (g) sources of information

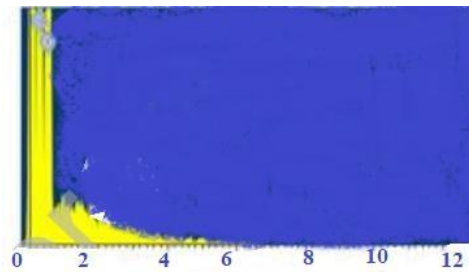
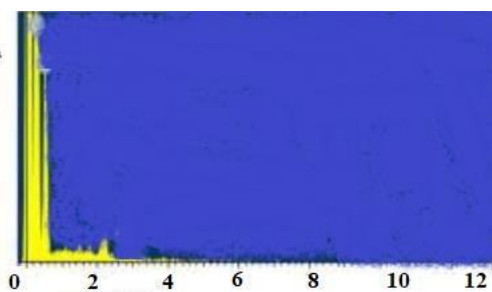
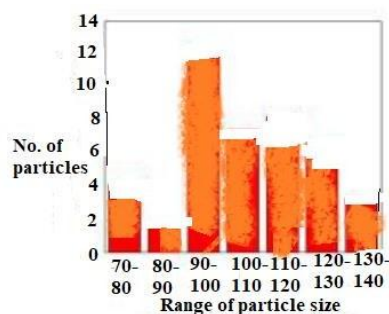
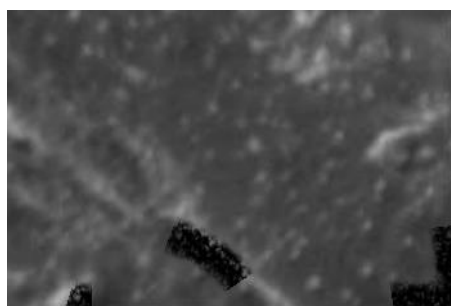
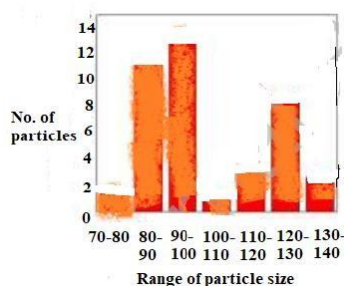
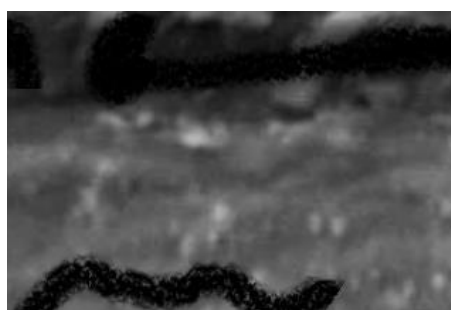


Fig. 2. a and b are two examples of examples of examples of example s of examples of examples of Ener gy-dispersive Xray (EDX) spectra are

visible in scanning electron microscope (SEM) d) micrographs C and d. Particle size distribution of chitosan nanocomposite fabrics (CNCFs) with in situ produced silver nanoparticles (AgNPs) using 1 mmol/L and 5 mmol/L aq. silver nitrite solutions, respectively, is shown in E and f

To examine their interaction, the FT-IR spectra of the chitosan fabric and the Vitex leaf extract are shown in Fig. 3a. In Fig. 3a, both spectra had the same apex, indicating that they belonged to the same chemical class. The apex of the matrix had a higher intensity than the chitosan textile at 3298  $\text{cm}^{-1}$  (OH stretching vibration) and 1012  $\text{cm}^{-1}$  (C-O-C stretching vibration), indicating that the leaf extract belonged to the OH and C-O-C categories. In order to investigate the effect of in situ generated silver nanoparticles on the chemical structure of the matrix, the FTIR spectra of the matrix and CNCFs using 15 mmol/L source solutions are shown in Fig. 3b. For coherence, the matrix and CNCF spectra using a 5 mmol/L origin solution are shown separately in Fig. 3c. With the exception of the overcasting of intensity of the bands corresponding to the O-H and C-O groups in the case of nanocomposite fabrics, no significant changes were seen in Figures 3b and 3c. The O-H and C-O classes of the matrix are definitely involved in converting silver salts to silver nanoparticles. Additional typical bands can be seen at 2898  $\text{cm}^{-1}$  (CH stretching.), 1633  $\text{cm}^{-1}$  (CH stretching.), and 1633  $\text{cm}^{-1}$  (CH stretching.). (CH stretching). (water crystallisation) At 1421  $\text{cm}^{-1}$  (CH<sub>2</sub> b.), 1352 and 1317  $\text{cm}^{-1}$  (CH<sub>2</sub> wagging), and 867  $\text{cm}^{-1}$  (CH<sub>2</sub> wagging), the chitosan structure is apparent in both the matrix and the CNCFs (-glucosidic linkage).

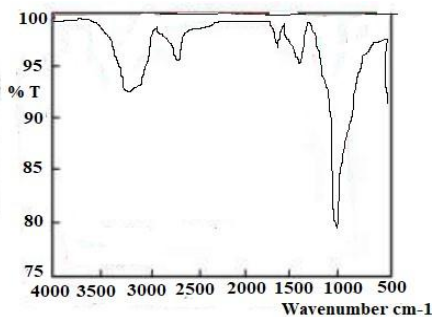
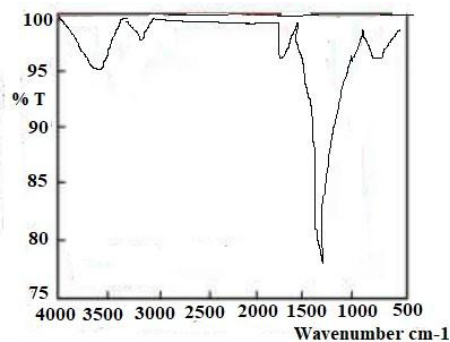
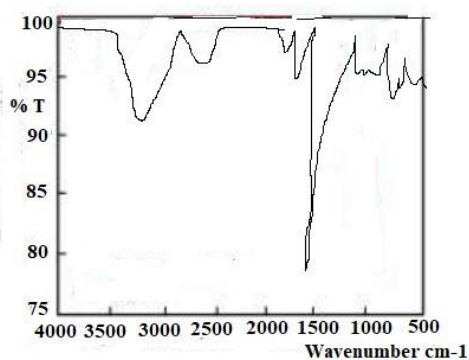


Fig.3: a) Chitosan fabric and matrix FTIR spectra; b) matrix and CNCFs with in situ produced Silver nanoparticles using 1–5 mmol/L aq. silver nitrite source solutions employing a 5 mmol/L source solution, a matrix and chitosan nanocomposite fabric with in situ produced silver nanoparticles. To investigate the effect of silver nanoparticles on the crystallinity of the nanocomposite fabrics, the X-ray diffractograms of the chitosan fibre, matrix, and nanocomposite chitosan fabrics among in situ generated silver nanoparticles using 1 to 5 mmol/L aq. silver nitrite solutions were described and shown in Fig. 4a. Because the overlapped diffractograms did not provide substantial information, the diffractograms communicate with the matrix and the CNCF utilising 5 mmol/L aq. Figure 4b depicts the various forms of silver nitrite solution. As seen in Fig. 4b, the CNCF intensity was somewhat greater than the matrix, indicating a minor increase in the crystallinity of the CNCFs due to the presence of silver nanoparticles.

Because the presence of silver nanoparticles in overlapped diffractograms is difficult to detect, the CNCF diffractogram using 5 mmol/L aq. silver nitrite was enlarged in  $2\theta = 30^\circ$  to  $67^\circ$  and is displayed in Fig. 4c. Figure 4c shows that the diffractograms of the peaks at  $2\theta = 39.1^\circ$ ,  $46.1^\circ$ , and  $64.2^\circ$  correspond to reflections from the (111), (200), and (220) planes of silver nanoparticles, respectively. Further prominent peaks can be found at  $2\theta = 33.0^\circ$ ,  $37.5^\circ$ ,  $57.2^\circ$ , and  $66.2^\circ$ , which correspond to reflections from the Ag-O nanoparticles planes (121), (209), (224), and (309), respectively. As a result, both silver nanoparticles and AgO nanoparticles were initiated in the CNCFs created. The in situ production of silver nanoparticles and AgO nanoparticles in the matrix is demonstrated by these results.

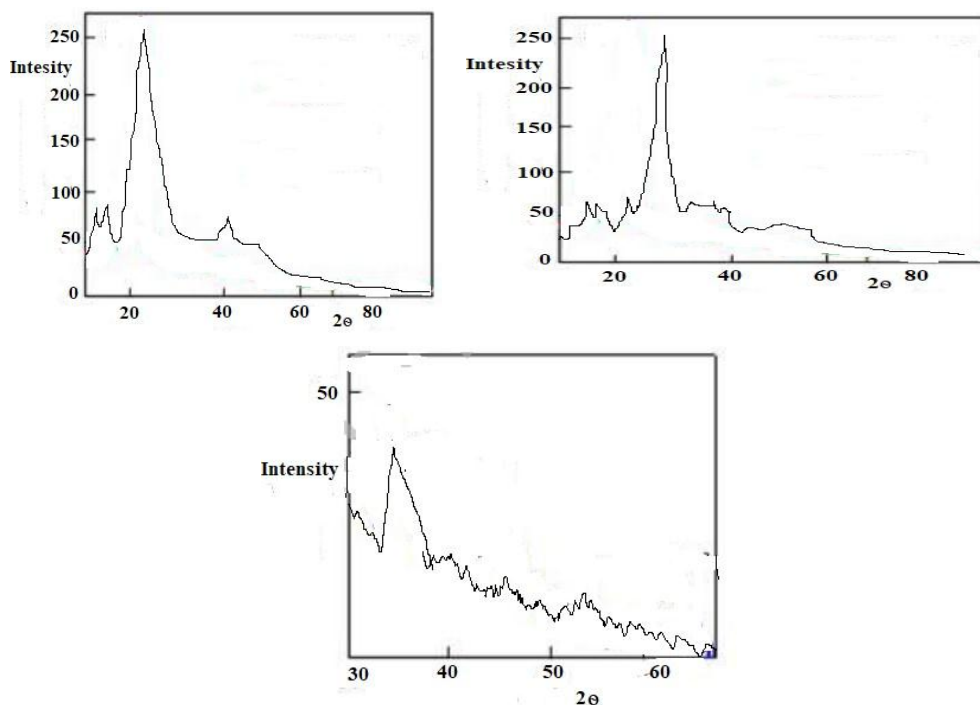


Fig.4. a) X-ray diffractograms (XRD) of chitosan fabric, matrix, and CNCFs produced with 1–5 mmol/L aq. Silver nitrite source solutions a) matrix and CNCF with a 5 mmol/L source solution b) and CNCF with a 5 mmol/L solution enlarged in the  $2\theta = 32^{\circ}$ – $68^{\circ}$  temperature range

The disc technique was used to test the antibacterial activity of the CNCFs produced using different concentrated source solutions against two gramme negative (*Pseudomonas* and *Escherichia coli*) and two gramme positive (*Bassilus subtilis* and *Staphylococcus aureus*) bacteria. A chitosan fabric and matrix comparative test was also performed. Images of the petri plates used in the experiment are shown in Fig. 5. Since the chitosan cloth and matrix were identified as A and B, the CNCFs using 1, 2, 3, 4, and 5 mmol/L were designated as H, I, J, K, and L in the images. Table 1 shows the diameter of the intelligible zones, which was computed using the Image J programme. As indicated in Fig.5 and Table 1, neither the chitosan cloth nor the matrix appears to have an antibacterial activity. Despite this, CNCFs between in situ started silver nanoparticles and Vitex leaf extract as a reducing agent demonstrated higher antibacterial activity against both gramme negative and gramme positive bacteria. In most cases, the comprehensible zone diameters ranged from 12.0 to 17.3 mm, and the concentration of the source solutions increased in all cases. CNCFs could be used as antibacterial materials in medicinal applications, according to these findings.

Table 1

Using 1–5 mmol/L aq. silver nitrite solutions against gramme negative (*Pseudomonas* and *Escherichia coli*) and gramme positive *Pseudomonas* and *Escherichia coli* bacteria, the diameter of the coherent zones was measured for chitosan fabric, matrix, and CNCFs (*Bassilus subtilis* and *Staphylococcus aureus*)

<u>Conc. Of</u> <u>aq. AgN</u> <u>O3 solution</u> <u>used</u>	<u>Diameter (mm)</u>			
	<u>E. coli</u>	<u>Pseudo</u> <u>monas</u>	<u>Staphylo</u> <u>coccus</u> <u>aureus</u>	<u>Bassil</u> <u>us su</u> <u>btilis</u>
Chitosan textile(A)	-	-	-	-
Matrix (B)	-	-	-	-
1 mmol/L (H)	12	13.3	12.6	13.7
2 mmol/L (I)	12.4	13.1	12.8	15.3
3 mmol/L (J)	14.7	14.8	14.4	16.1
4 mmol/L (K)	15.6	14.8	15.6	15.7
5 mmol/L (L)	15	15.9	17.9	14.2

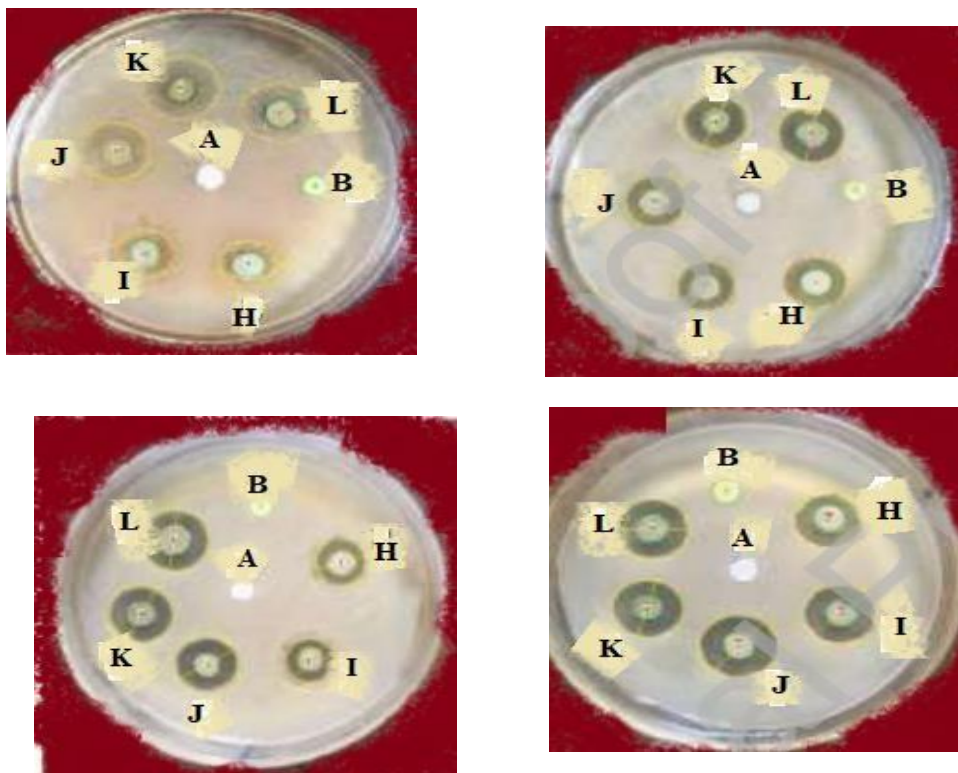


Fig. 5. CNCFs with in situ generated AgNPs using 1 mmol/L (H), 2 mmol/L (I), 3 mmol/L (J), 4 mmol/L (K), and 5 mmol/L (L) aq; antibacterial activity of chitosan fabric (A); matrix (B); CNCFs with in situ generated AgNPs using 1 mmol/L (I), 3 mmol/L (J), 4 mmol/L *Pseudomonas aeruginosa* (a), *Escherichia coli* (b), *Bacillus subtilis* (c), and *Staphylococcus aureus* (d) bacteria were tested using  $\text{AgNO}_3$  source solutions and Vitex leaf extract as a reducing agent.

## References

1. Zagho M., Hussein E.A., Elzatahry A. Recent Overviews in Functional Polymer Composites for Biomedical Applications. *Polymers*. 2018; 10: 739.
2. Sherif G., Chukov D.I., Tcherdyntsev V., Torokhov V. Effect of Formation Route on the Mechanical Properties of the Polyethersulfone Composites
3. Mustafa A., Bin Abdollah M.F., Shuhimi F.F., Ismail N., Amiruddin, H. Umehara N. selection and verification of kenaf fibres as an alternative friction material using Weighted Decision Matrix method. *Mater. Des.* 2015; 67:577–582.
4. Capadona J. R., Van Den Berg O., Capadona L. A., Schroeter M., Rowan S. J., Tyler D. J., & Weder C. A versatile approach for the processing of polymer nanocomposites with self-assembled nanofibre templates. *Nature Nanotechnology*. 2007; 2: 765-769.
5. Mark JE. Ceramic-reinforced polymers and polymer-modified ceramics. *Polymer Engineering & Science*. 1996;36 (24):2905-20.

6. Huang H., Yuan Q., Yang X. Preparation and characterization of metal-chitosan nanocomposites. *Colloids and surfaces B: Biointerfaces*. 2004;39(1-2):31-7.
7. Akamatsu K., Takei S., Mizuhata M., Kajinami A., Deki S., Takeoka S., Fujii M., Hayashi S., Yamamoto K. Preparation and characterization of polymer thin films containing silver and silver sulfide nanoparticles. *Thin Solid Films*. 2000 ;359(1):55-60.
8. Zeng R., Rong MZ., Zhang MQ., Liang HC., Zeng HM. Laser ablation of polymer-based silver nanocomposites. *Applied Surface Science*. 2002;187:(3-4):239-47.
9. Cole DH., Shull KR., Baldo P., Rehn L. Dynamic properties of a model polymer/metal nanocomposite: gold particles in poly (tert-butyl acrylate). *Macromolecules*. 1999;32(3):771-9.
10. Hussain I., Brust M., Papworth A J., Cooper AI. Preparation of acrylate-stabilized gold and silver hydrosols and gold-polymer composite films. *Langmuir*. 2003;19(11):4831-5.
11. Vijaya Kumar R., Elgamiel R., Diamant Y., Gedanken A., Norwig J. Sonochemical preparation and characterization of nanocrystalline copper oxide embedded in poly (vinyl alcohol) and its effect on crystal growth of copper oxide. *Langmuir*. 2001;17(5):1406-10.
12. Sajinovic D, Saponjic ZV, Cvjeticanin N, Marinovic-Cincovic M, Nedeljkovic JM. Synthesis and characterization of CdS quantumdot/polystyrene composite. *Chemical Physics Letters*. 2000;329(1-2):168-72.
13. Djokovic V, Nedeljkovic JM. Stress relaxation in hematite nanoparticles-polystyrene composites. *Macromolecular rapid communications*. 2000 ;21(14):994-7.
14. Kumar RV., Kolytyn Y., Cohen YS., Cohen Y., Aurbach D., Palchik O., Felner I., Gedanken A. Preparation of amorphous magnetite nanoparticles embedded in polyvinyl alcohol using ultrasound radiation. *Journal of Materials Chemistry*. 2000;10(5):1125-9.
15. Yu SH., Yoshimura M., Calderon Moreno JM., Fujiwara T., Fujino T., Teranishi R. In situ fabrication and optical properties of a novel polystyrene/semiconductor nanocomposite embedded with CdS nanowires by a soft solution processing route. *Langmuir*. 2001;17(5):1700-7.
16. Croce F., Appetecchi GB., Persi L, Scrosati B. Nanocomposite polymer electrolytes for lithium batteries. *Nature*. 1998 ;394(6692):456-8.
17. Huynh WU., Peng X., Alivisatos AP. CdSe nanocrystal rods/poly (3-hexylthiophene) composite photovoltaic devices. *Advanced materials*. 1999 ;11(11):923-7.
18. Guo L., Yang S., Yang C., Yu P., Wang J., Ge W., Wong GK. Synthesis and characterization of poly (vinylpyrrolidone)-modified zinc oxide nanoparticles. *Chemistry of Materials*. 2000 ;12(8):2268-74.
19. Zhao M., Sun L., Crooks RM. Preparation of Cu nanoclusters within dendrimer templates. *Texas A and M University college station dept of chemistry*. 1998.
20. Esumi K., Suzuki A., Yamahira A., Torigoe K. Role of poly (amidoamine) dendrimers for preparing nanoparticles of gold, platinum, and silver. *Langmuir*. 2000;16(6):2604-8.

21. Zheng J., Stevenson MS., Hikida RS., Van Patten PG. Influence of pH on dendrimer-protected nanoparticles. *The Journal of Physical Chemistry B*. 2002;106(6):1252-5.
22. Huang H., Yuan Q., Yang X. Preparation and characterization of metal-chitosan nanocomposites. *Colloids and Surfaces B: Biointerfaces*. 2004;39(1-2):31-7.
23. Fuentes S., Retuert PJ., Ubilla A., Fernandez J., Gonzalez G. Relationship between composition and structure in chitosan-based hybrid films. *Biomacromolecules*. 2000;1(2):239-43.
24. Tanabe T., Okitsu N., Tachibana A., Yamauchi K. Preparation and characterization of keratin-chitosan composite film. *Biomaterials*. 2002;23(3):817-25.
25. Zhang M., Li XH., Gong YD., Zhao NM., Zhang XF. Properties and biocompatibility of chitosan films modified by blending with PEG. *Biomaterials*. 2002;23(13):2641-8.
26. Sadanand V., Rajini N., Varada Rajulu A., Satyanarayana B. Preparation of cellulose composites with in situ generated copper nanoparticles using leaf extract and their properties. *Carbohydr. Polym.* 2016;150:32-39.
27. Jamshidi A., Jahangiri M. Synthesis of copper nanoparticles and its antibacterial activity against *Escherichia coli*. *Asian J. Biol. Sci.* 2014; 7:183-186